

# Advanced System-on-Package (SOP) Front-End Passive Solutions for RF and Millimeter-Wave Wireless Systems

J.-H.Lee<sup>(1)</sup>, L.Marcaccioli<sup>(2)</sup>, G.Dejean<sup>(1)</sup>, C. Lugo<sup>(1)</sup>, S.Pinel<sup>(1)</sup>, J.Papapolymerou<sup>(1)</sup>, J.Laskar<sup>(1)</sup>, R.Sorrentino<sup>(2)</sup> and M.M.Tentzeris<sup>(1)</sup>

<sup>(1)</sup>School of ECE, Georgia Institute of Technology, Atlanta, GA 30332-250, U.S.A..

<sup>(2)</sup> University of Perugia, Dept. of Electronic and Information Engineering, 06125 Perugia, Italy  
e-mail: jonglee@ece.gatech.edu

**Abstract**— In this paper, we present novel three-dimensional (3-D) compact and easy-to-design passive solutions (filters/duplexers, antennas, couplers) using system-on-package (SOP) multilayer low temperature cofired ceramic (LTCC) and organic (Liquid Crystal Polymer (LCP)) technologies in RF and millimeter-wave wireless systems. Both ceramic and organic technologies are candidates for the 3-D integration of system-on-package (SOP) miniaturized RF/microwave/millimeter-wave systems. LTCC has been widely used as a packaging material because of its process maturity/stability and its relatively high dielectric constant that enables a significant reduction in the module/function dimensions. As an alternative, LCP is an organic material that offers a unique combination of electrical, chemical, and mechanical properties, enabling high-frequency designs due to its ability to act as both the substrate and the package for flexible and conformal multilayer functions. A compact LTCC single-mode patch resonator filter utilizing vertical coupling overlap and transverse cuts as design parameters has been designed at operating frequency band of 58-60GHz. Then, a compact transmit/receive duplexer (39.8GHz/59GHz) has been realized by the noble 3D deployment of the presented single-mode patch resonators to provide low insertion loss and high channel-to-channel isolation. A double fed cross-shaped microstrip antenna has been designed for the purpose of doubling the data throughput by means of a dual-polarized wireless channel, covering the band between 59-64 GHz. This antenna can be easily integrated into a wireless millimeter-wave link system. Finally, a new architecture concept intended for reconfigurable couplers is proposed. The device has been fabricated and tested in microstrip technology at 5 GHz. The novel concept introduced is independent of the used technology; a multilayer 35 GHz version in LCP substrate, meant to be used with MEMS switches, has also been designed and simulated.

**Index Terms** – patch resonator, duplexer, low-temperature cofired ceramic (LTCC), intelligent system-on-package (SOP), 3D/vertical integration, microstrip antenna, millimeter-wave (mmW), reconfigurable coupler, MEMS.

## I. INTRODUCTION

The rapid expansion of wireless communications and personal communication networks has led to tremendous demands of miniaturization, portability, low-manufacturing cost and high performance in RF and millimeter-wave (mmW) wireless systems [1]. The RF front-end module is the foundation of these systems and its integration poses rigid challenges in terms of

high performance up to 100 GHz operating frequency, large number of embedded passive components, low power consumption and compactness. To fulfill these primary requirements, RF and millimeter-wave design and packaging have been established for decades as key technologies and developed to realize more flexible and reconfigurable systems for emerging high-performance applications such as personal communication networks, short-range broadband wireless local area networks (WLAN) and RF-optical networks. Although several packaging approaches have been investigated to integrate the front-end components, such as a monolithic microwave integrated circuit (MMIC) chipset (low-noise and power amplifiers, up-and-down mixers, voltage-controlled oscillator...) and passive functions (antennas, filters, couplers...), the system-on-Package (SOP) approach has emerged as the effective solution to provide a high level of integration because it offers not only great capability of integrating embedded functions, but also the real estate efficiency and cost-saving [1]. In addition, the recent development of multilayer materials and processes in packaging area makes SOP to be a candidate solution for ever higher frequency miniaturized front-end modules [2].

Our paper focuses mainly on advanced multilayer organic substrates such as Liquid Crystal Polymer (LCPs), as well as low-temperature cofired ceramics (LTCCs). The very mature fabrication capabilities of LTCC ( $\epsilon_r=5.4$ ,  $\tan\delta=0.0015$ ) up to 100 GHz enable the replacement of broadside coupling by vertical coupling and make LTCC a competitive solution to meet millimeter wave design requirements. Also multilayer capability of up to 20 metal layers makes LTCC attractive for 3-D integrated components as filters and antennas in a compact and cost-effective manner. As an alternative, Liquid Crystal Polymer (LCP) is an organic material that offers a unique low-cost all-in-one solution for high frequency designs due to its ability to act as both a high-performance flexible substrate ( $\epsilon_r=2.9-3.0$ ,  $\tan\delta=0.002-0.004$ ) and a near-hermetic package for multilayer modules [2-4]. These characteristics make LCP very appealing for many applications and it can be viewed as another prime technology for enabling system-on-package RF and millimeter-wave (mmW) designs [2]. The choice of the most suitable technology depends on the application specifications such as environment, operation frequency, performance, volume and cost.

In this paper, we address the development of various advanced 3-D LTCC and LCP system-on-package passive

components as the candidates of choice for 3-D integration of compact, low cost wireless front-end systems to be used in RF and up to V-band frequency ranges. The single-mode slotted patch resonator filters with a transverse cut on each side first have been exploited at the operating frequency band of 58-60 GHz of mobile communication systems to achieve compactness and great compromise between size and power handling. After ensuring their performances with measurement data, the compact multilayer transmit/receive duplexers have been presented to cover two bands (39.8 GHz/59GHz) of dual-band mobile communication systems with low insertion loss and high channel-to-channel isolation. A cross-shaped antenna has been designed for a dual-polarized transmission and reception of signals that cover the band between 59-64 GHz, in a configuration that can be easily integrated into wireless millimeter-wave transmit/receive modules. The last developed device is a reconfigurable coupler. The structure proposed is a new architecture that can be implemented in several different technologies, the reconfigurability being obtained by means of MEMS switches or PIN diodes. In the present work, a microstrip hardwired prototype operating at 5 GHz has been fabricated and tested, in order to demonstrate the concept introduced. A scaled multilayer version at 35 GHz, in LCP substrate, has also been designed and fabrication is currently under way.

## II. PATCH RESONATOR FILTER/DUPLEXER ON LTCC

The band pass filters and duplexers are core passive components that can be easily integrated into RF and millimeter-wave front-ends. On-package multilayer filters/duplexers offer a very attractive implementation in terms of both a high-level of integration and reduction of assembly cost. In this section, the design of a single-mode slotted patch filter [5-6] is presented for two operating frequency bands (38-40 GHz and 58-60GHz). Then, multilayer duplexers are realized for V-band transmit/receive systems to isolate any power transmit stage from sensitive receive stages sharing a common antenna. All designs have been simulated using the MOM-based, 2.5D full-wave solver IE3D and fabricated in LTCC ( $\epsilon_r=5.4$ ,  $\tan\delta=0.0015$ , 11 substrate layers (each layer thickness: 100  $\mu\text{m}$ )).

Figure 1 shows the top view ( $L \times L = 0.616 \text{ mm} \times 0.616 \text{ mm}$ ) of the proposed single-mode slotted patch resonator filter with a transverse cut on each side for 58-60 GHz applications such as short-range broadband WLAN. The side view and photograph of the resonators are shown in figures 2 and 3, respectively. The patch filter is designed to achieve 3% 3-dB bandwidth, <3dB insertion loss and the center frequency of 60 GHz. Such a structure has been developed from the basic half-wavelength ( $\lambda/2$ ) square patch resonator. In order to maximize the coupling strength between the feeding structures and the patch, while minimizing the effect of the fabrication, the proposed novel structure takes advantage of the vertical development filter elements by inserting the feedlines (M2) and the resonator (M3) into different metal layers as shown in figure. 2. This transition introduces a 7.6 % frequency downshift because of the additional capacitance effect as compared to the basic  $\lambda/2$  square patch resonator directly attached by feedlines.

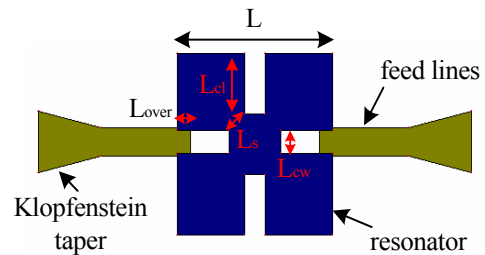


Figure 1. Top view of Miniaturized 60GHz slotted patch resonator.

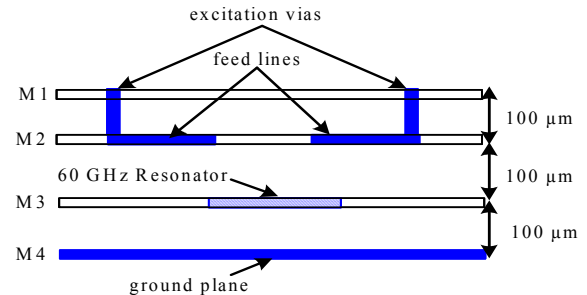


Figure 2. Side view of 60GHz slotted patch resonator.

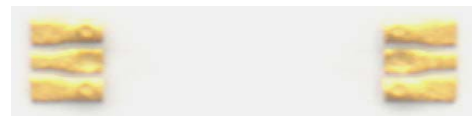


Figure 3. The photographs of fabricated filters with coplanar waveguide (CPW) pads at 60GHz.

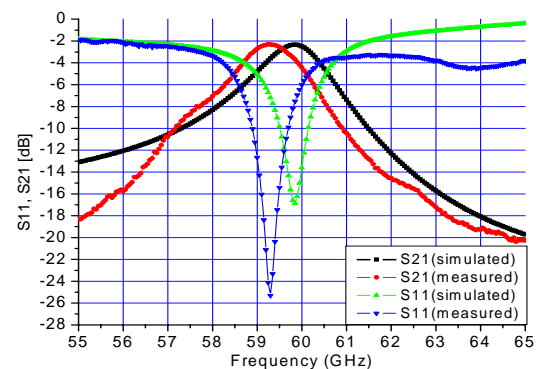


Figure 4. Measured and simulated S-parameters of 60 GHz slotted patch resonator.

Transverse cuts have been added on each side of the patch and contribute to significant miniaturization of its size due to additional inductance effects. The operating frequency range shifts downward about 33 % as the length of the cut ( $L_{cl}$  in Fig. 1) increases by approximately 379  $\mu\text{m}$  while the width of the cuts ( $L_{cw}$  in Fig. 1) is fixed to  $L/8$  determined by the fabrication tolerance. Additional miniaturization is limited by the minimum distance ( $L_s$  in Fig. 1) between the corners of adjacent orthogonal cuts.

The patch size is significantly reduced from  $\lambda/2$  to 0.616 mm. The degradation of bandwidth due to patch's miniaturization can be improved by adjusting the overlap distance ( $L_{ov}$  in Fig. 1) between the resonator and the feedlines that directly affects the external quality factor ( $Q_{ext}$ ).

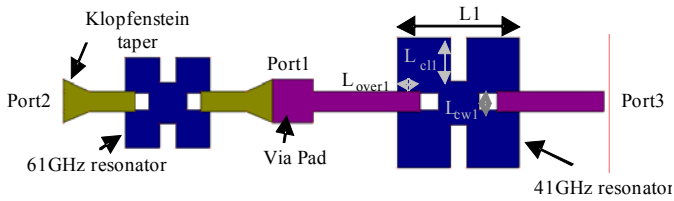


Figure 5. Top view of the dual-band compact duplexer (41GHz/61GHz) consisting two patch resonators connected together with a via junction.

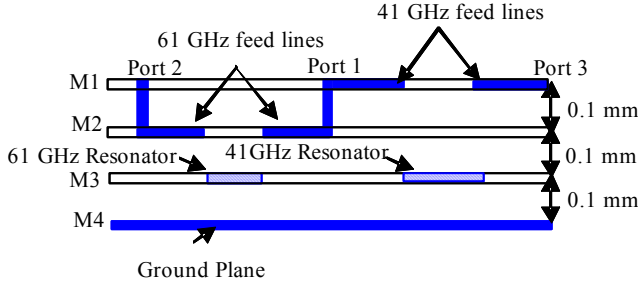


Figure 6. Side view of the dual-band compact duplexer (41GHz/61GHz) in multilayer configuration.

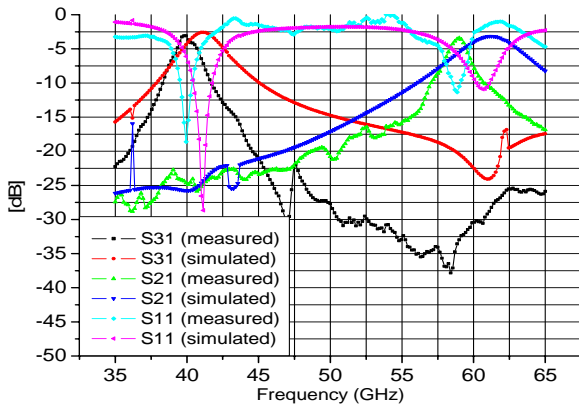


Figure 7. Measured and simulated insertion loss (Channel1:S31, Channel:S21) and return loss (S11) for both channels of duplexer.

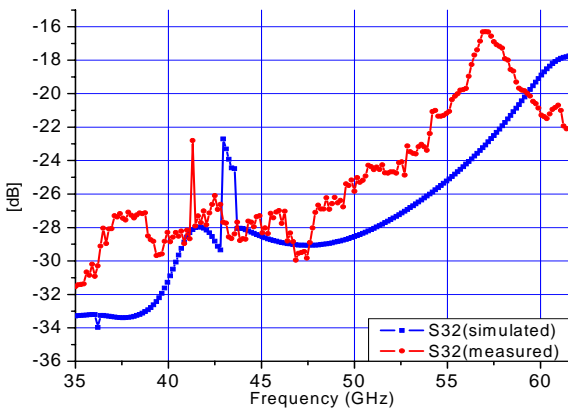


Figure 8. Measured and simulated channel to channel isolation (S32).

The proposed embedded microstrip line filters are excited through via connecting waveguide signal pads on the top metal layer (M1 in Fig. 2), reducing radiation loss compared to microstrip type filter on the top (surface) layer. The overlap ( $L_{over} \sim L/31$ ) and transverse cuts ( $L_{cw} \sim L/8$ ,  $L_{cl} \sim L/3.26$ ) have

been finally determined to achieve desired filter characteristics with the aid of IE3D.

The overall size is  $4.018 \text{ mm} \times 1.140 \text{ mm} \times 0.3 \text{ mm}$  including the CPW measurement pads. Figure 4 shows that the experimental results of the filter agree very well with the simulation data. It can be easily observed that the insertion loss is  $< 2.3 \text{ dB}$ , the return loss  $> 25.3 \text{ dB}$  over the pass band and the 3dB bandwidth is about 1 GHz. The center frequency shift from 59.85 GHz to 59.3 GHz can be attributed to the fabrication accuracy (vertical coupling overlap affected by the alignment between layers, layer thickness tolerance). This was the first fabrication iteration and the differences could be corrected in the second and third iterations.

With the development of the miniaturized patch resonators, the compact transmit/receive duplexers are designed around the 41/61GHz center frequencies (channel1/channel2) with  $< 3 \text{ dB}$  insertion loss for both channels, and 6% 3-dB bandwidth to cover two bands of interest (41/61GHz) for mobile communications. The top and side views of the topology chosen for the duplexer are shown in figure 5 and 6, respectively. A via junction which constitutes the common input (Port 1 in Fig.5) is utilized to connect the two resonant patch filters. The 61 GHz patch filter occupies the left portion of the duplexer, while the 41 GHz filter the right portion as shown in figure 6. The feedlines of the 41 GHz patch filter are placed on the top metal layer (M1 in Fig. 6) not only to obtain the desired coupling coefficient between the feedlines and the 41GHz resonator but also to realize the compact 3-D multilayer duplexer configuration occupying only three substrate layers. The overlap ( $L_{over}$  in Fig. 5) works as main control-factor to improve the bandwidth and has been determined to  $L/8.3$  for a fixed dimension of the transverse cuts ( $L_{cw1} \sim L/8.2$ ,  $L_{cl1} \sim L/3$ ) with aid of IE3D. The slot length ( $L_{cl1}$  in fig7) is determined to fulfill target the insertion and center frequency specifications in the same way as the section A. The fabricated duplexer occupies an area of  $5.719 \times 1.140 \times 0.3 \text{ mm}$  including the CPW measurement pads and the CPW-microstrip transition.

The simulated and measured insertion and return losses of the duplexer (channel1/channel2) are compared in figure 7. The measured insertion losses (3.1/3.4 dB) for both channels are slightly higher than the simulated values while the return losses (18.6/11.32dB) decrease from the theoretical values (27/18dB). The measured bandwidths (4.8/3.25%) over both channels are narrower than the simulation results (5.2/6%). Also, the center frequency downshift is commonly observed for both channels. The discrepancy between the simulated and measured insertion/return loss values can be attributed to the fabrication accuracy of the feeding line /cut designs that have been computationally optimized for the original resonant frequencies and not for the shifted frequencies. In addition, the narrower bandwidth in measurements compared to the simulations might be due to the fabrication accuracy of the vertical-coupling overlap design that is optimized for the original resonant frequencies and not for the shifted frequencies. The measured isolation (Fig. 8) agrees fairly well

with the simulated values. Overall isolation is -29.5 dB at 39.8 GHz, -20.4 dB at 59 GHz and better than -16.3 dB in the worst case.

### III. CROSS-SHAPED MICROSTRIP ANTENNA FOR MILLIMETER-WAVE APPLICATIONS

A cross-shaped antenna has been designed for the transmission and reception of signals that covers the entire frequency band between 59-64 GHz. This antenna can be easily integrated within a wireless millimeter-wave module containing the components of the previous section. Its structure is dual-polarized for the purpose of doubling the data output rate transmitted and received by the antenna. The cross-shaped geometry was utilized to decrease the cross-

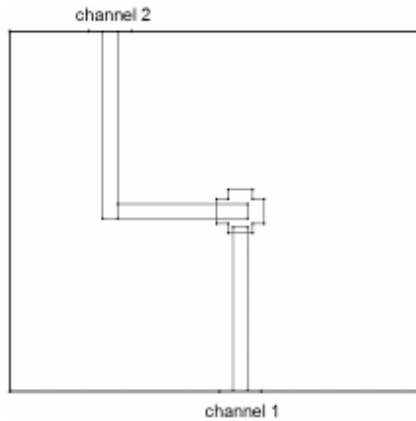


Figure 9. Antenna Structure.

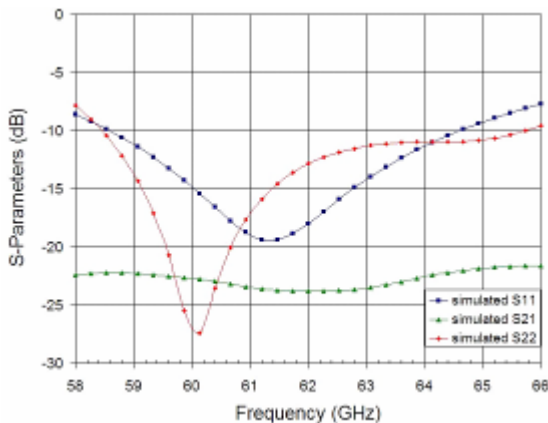


Figure 10. Simulated S-Parameter data versus frequency

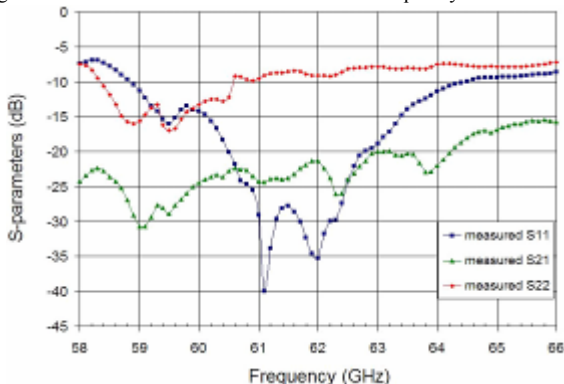


Figure 11. Measured S-Parameter data versus frequency

polarization which contributes to unwanted side-lobes in the radiation pattern [7].

The antenna, shown in Fig.9, was excited by proximity-coupling and had a total thickness of 12 metal layers and 11 substrate layers (each layer was 100  $\mu\text{m}$  thick). Proximity-coupling is a particular method for feeding patch antennas where the feedline is placed on a layer between the antenna and the ground plane. When the feedline is excited, the fringing fields at the end of the line strongly couple to the patch by electromagnetic coupling. This configuration is a non-contact, non-coplanar method of feeding a patch antenna. The use of proximity-coupling allows for different polarization reception of signals that exhibits improved cross-channel isolation in comparison to a traditional coplanar microstrip feed. There were two substrate layers separating the patch and the feedline, and two substrate layers separating the feedline and the ground layer. The remaining seven substrate layers are used for burying RF circuitry beneath the antenna that includes the filter, integrated passives and other components. The size of the structure was 8mm $\times$ 7mm. A right angle bend in the feedline of channel 2 is present for the purpose of simplifying the scattering parameter measurements on the network analyzer.

The design was simulated using the TLM-based, 3D full-wave solver MicroStripes 6.0. Fig. 10 shows the simulated scattering parameters versus frequency for this design. The targeted frequency of operation was around 61.5 GHz for both channels. The simulated return loss for channel 1 (S11) was approximately -19dB at  $f_r = 61.5$  GHz, while for channel 2 (S22), the return loss was  $\sim$  -27.5dB at  $f_r = 60.1$  GHz. The simulated resonant frequencies for both channels were optimized in order to cover the desired band based on the antenna structure. It is worth noting the resonant frequency of channel 2 is intentionally shifted to the left of the targeted frequency of operation. This is due to the existence of a parasitic resonance at 64.24 GHz that has a return loss of  $\sim$  -11 dB. For the feed at channel 2, the bandwidth achieved by the  $\text{TM}_{10}$  mode, was hindered by the discontinuity in the feedline, but by adjusting the feed point at the end of the feedline to a different position, a parasitic resonance is brought closer to the  $\text{TM}_{10}$  resonance. By taking advantage of both resonances, the required band is achieved. Channel 2 has a wider bandwidth (12.15%) than that of channel 1 (9.76%) primarily due to the right angle bend in the feedline and the combination of the  $\text{TM}_{10}$  mode (resonant at a lower frequency) and the parasitic resonance. The bandwidth is recorded at -10 dB.

Fig. 11 also shows the measured scattering parameters versus frequency for the design. The measured return loss for channel 1 (-40dB @  $f_r = 61.1$  GHz) is better than that obtained through the simulation (-19dB). Conversely, the -17dB of measured return loss at  $f_r = 59.5$  GHz obtained for channel 2 is worse than the simulated return loss of -27.5dB. The enhanced return loss of channel 1 may be due to parasitic effects associated with measurement equipment (cables, connectors, etc...). The diminished return loss of channel 2 could result from

measurement inaccuracies or constructive interference of parasitic resonances at or around the  $TM_{10}$  resonance. The asymmetry in the feeding structure may account for this difference in the measured return loss. Although frequency shifts for both channels are present in the measured return loss plots, these shifts are insignificant at 60 GHz and above. Additionally, the measured bandwidth of channel 1 (9.00%) is slightly narrower than that seen in the simulation (9.76%). Some measurement inaccuracies may attribute in this small deviation. On the other hand, the bandwidth for channel 2 (3.70%) is significantly narrower than the simulated bandwidth (12.15%). This is due to the diminished return loss in the measurement that played a major role in narrowing the bandwidth. It is worth noting that the bandwidth at -8 dB is 9.41% (between 58.2 – 63.8 GHz) which would cover the 5GHz band between 59-64 GHz if the resonant frequency was shifted to the right. The simulated cross-coupling (S21) between channels 1 and 2 (Fig. 10) is below -22 dB for the required bands. On the other hand, the measured cross-coupling between the channels is below -20dB for the required bands. Due to the close proximity of the feeding line terminations of the channels, the cross-coupling is slightly hindered, but these values are satisfactory for this application.

#### IV. RECONFIGURABLE COUPLER

To further minimize the size of the SOP-based RF front-ends, it is critical to integrate multifunctional and reconfigurable devices in order to cover effectively many standards and frequency bands (e.g. cognitive radio, smart front-ends). As a proof of concept of this approach, a SOP-integrated 3D reconfigurable coupler using MEMS or PIN diodes is presented. The basic idea is to use an additional line – with respect to a standard two line coupler – which can be either connected to one of the main signal lines or left floating.

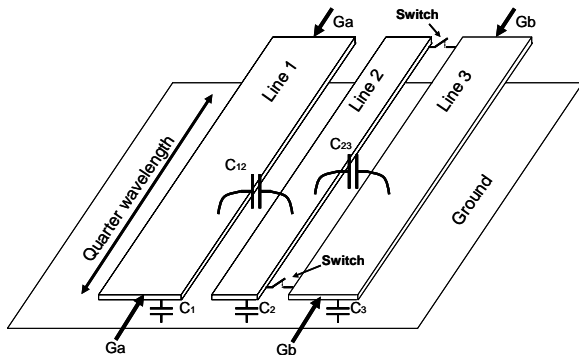


Figure 12. Three line asymmetrical coupler, scheme proposed.  $G_a$ ,  $G_b$ : terminating admittances.

Referring to Fig.12, which is a planar configuration of the concept introduced, the device toggles its state between two configurations: when both switches are on – ideally a short circuit, the middle line is shunted to one of the two side lines. A strong coupling is therefore obtained by means of the proximity of line 1 and line 2. On the other hand, when the switches are off, the middle line is floating and, being line 1 and line 3 farther, the coupling is weaker. In both cases the device must

exhibit good matching and high isolation. The design procedure is based on the formula provided by Cristal in [9], where an asymmetrical two-line coupler has been proposed for the first time, but for brevity it is not reported in this paper.

By cascading the basic design shown in fig. 12 - provided that the overall distance end-to-end is a quarter of a wavelength - it is possible to design reconfigurable couplers with any number of bits, with several different coupling levels as well. Each bit is enabled by two switches, which are simultaneously “ON” or “OFF”. In order to demonstrate the concept introduced, one 2-bit reconfigurable microstrip coupler has been designed and measured, at a center frequency of 5.2 GHz.

In this first prototype, the switches have been replaced by hardwired connections (ideal short/open); therefore four samples, corresponding to the four possible states, have been constructed. In Fig. 13 it is possible to see one of the fabricated boards. The results, shown in Fig. 14, show a directivity of more than 15 dB and reflection losses of less than -15 dB in the operating frequency band.

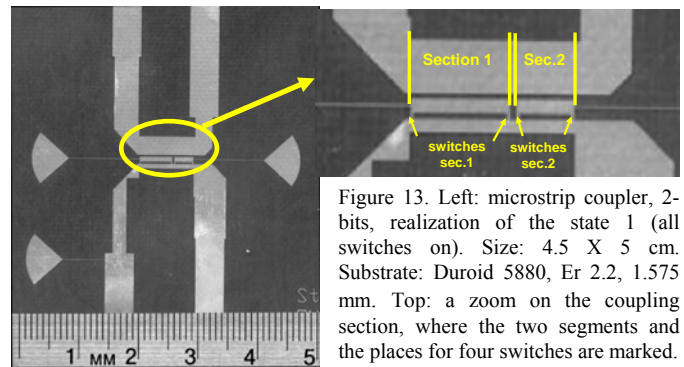


Figure 13. Left: microstrip coupler, 2-bits, realization of the state 1 (all switches on). Size: 4.5 X 5 cm. Substrate: Duroid 5880, Er 2.2, 1.575 mm. Top: a zoom on the coupling section, where the two segments and the places for four switches are marked.

The power losses have been calculated to be less than 0.6 dB. If PIN diodes are added, the losses are expected to increase to about 1.5 dB in the worst case (all switches on, state 1), but they will be significantly less if MEMS are used.

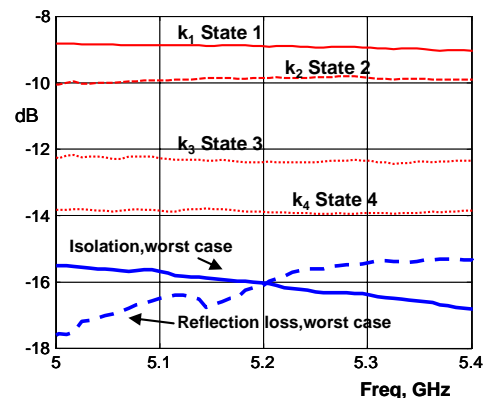


Figure 14. Measured results in the band of interest (5 to 5.4 GHz). Coupling ratio: -8.5, -10, -12, -14 dB. Reflection losses (dotted line): <-15 dB. Isolation (solid line): <-15 dB.

Microstrip technology can only be used to construct side by side coupler, thus only with low-level coupling ratio. A broadside configuration is doubtlessly more effective to increase the coupling of the structure. A two-layer design has

therefore been carried out at a center frequency of 35GHz. The principle is the same already described, and the design can be seen in Fig.15-16. The signal flows in different layers in line 1 and 2, while the line 3, open-ended, is used to enhance the coupling, the structure being in the latter case equivalent to an asymmetrical broadside coupler. In this first design, there are 2 states only (one bit), and LCP substrate has been used ( $\epsilon_r = 3.16$ ,  $\tan\delta = 0.0043$ ) [10]. The results, shown in Fig.17, are obtained by simulations, and the fabrication is in progress.

Observe that the coupling ratio ranges from -3 to -9.5 dB, and an isolation and reflection losses of less than -23 dB are obtained.

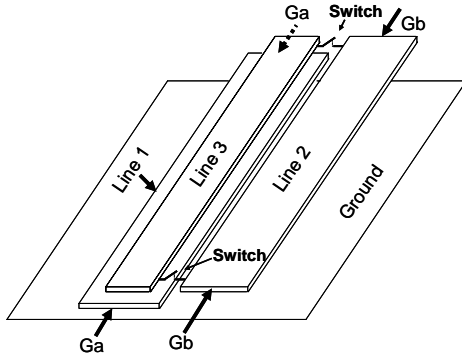


Figure 15. Perspective view of a two-layer coupler scheme in LCP substrate.

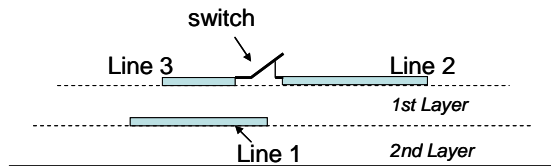


Figure 16. Transverse view of the coupler of Fig.17. Two layers make possible to strongly enhance the coupling – when required – between line 1 and line 3. Thickness layer 1: 3mil. Thickness layer 2: 4 mil.

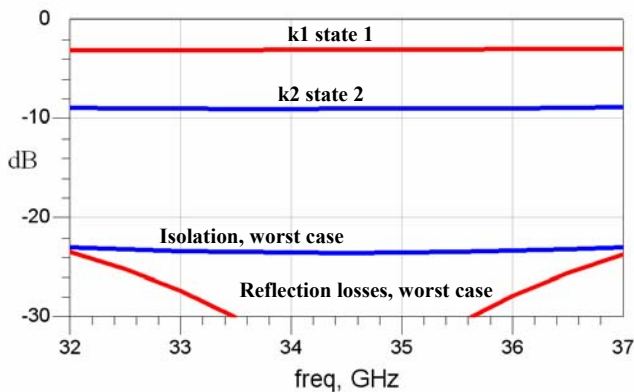


Figure 17. Results (simulation) of the 2-layer coupler of Fig. 17-18.

## V. CONCLUSIONS

A new class of compact and highly integrated passive functions, such as filters/duplexers, antennas and couplers, has been demonstrated to enable a complete passive solution for compact, low cost, wireless reconfigurable RF and millimeter-wave front-end systems in both multilayer LTCC and LCP technology. The LTCC patch resonator filter that uses vertical coupling overlap and transverse cuts as design

parameters achieves a high level of miniaturization. Excellent performance is verified at the operating frequency of 59.3 GHz through a measured insertion loss of  $< 2.3$  dB and a return loss of  $> 25.3$  dB over the pass-band, and a bandwidth of 1.67%. On the basis of the single-mode patch resonators, a multilayer compact duplexer has been realized by the noble 3D deployment of the presented single-mode patch resonators and demonstrated low insertion loss and high channel-to-channel isolation over two operating frequency channels (39.8GHz/59GHz) suitable for V-band mobile communication and inter-satellite applications. A double fed cross-shaped microstrip antenna has been designed for the purpose of doubling the data throughput by means of a dual-polarized wireless channel, covering the band between 59-64 GHz. This antenna can be easily integrated into a wireless millimeter-wave link system. Finally, a new architecture concept intended for reconfigurable couplers has been proposed. The device can be reconfigured by means of RF MEMS switches or PIN diodes; a multilayer LCP version has been designed and simulated at 35GHz. The compactness and the low losses associated with this kind of structure makes it particularly suitable for intelligent SOP RF modules.

## ACKNOWLEDGMENTS

The authors wish to acknowledge the support of Asahi Glass Co., the Georgia Tech., Packaging Research Center, the Georgia Electronic Design Center, the NSF Career Award #ECS-9984761, and the NSF Grant #ECS-0313951.

## REFERENCES

- [1] M. M.Tentzeris, et al. "3-D Integrated RF and Millimeter-Wave Functions and Modules Using Liquid Crystal Polymer (LCP) System-On-Package Technology," *IEEE Transactions on Advanced Packaging*, Vol.27, No.2, May 2004, pp.332-340.
- [2] S.Pinel, et al. "High-Q Passives on Liquid Crystal Polymer Substrates and BGA Technology for 3D Integrated RF Front-end Module," *IEICE Trans. on Electronics*, Vol. E86-C, No. 8, Aug. 2003, pp 1584-1592.
- [3] M.F. Davis, et al. "Integrated RF Function Architectures in Fully-Organic SOP Technology", in *2001 IEEE Electrical Performances of Electronic Packaging Conference*, Cambridge, Massachusetts, Oct. 2001, pp 93-96.
- [4] Kellee Brownlee, Swapan Bhattacharya, Ken-ichi Shinotani, CP Wong and Rao Tummala, "Liquid Crystal Polymer for High Performance SOP Applications", in *2002 IEEE International Symposium on Advanced Packaging Materials*, pp 249-253.
- [5] V.Kondratyev, M.Lahti, and T.Jaakola, "On the design of LTCC filter for millimeter-waves," in *2003 IEEE MTT-S Int. Microwave Sym. Dig.*, Philadelphia, PA., June 2003, pp. 1771-1773.
- [6] J.-H.Lee, et al. "Advanced 3-D LTCC system-on-package (SOP) architectures for highly integrated millimetre-wave wireless systems," presented at *Proc. 34th EuMC*, Amsterdam, Nederland, 2004.
- [7] A.Tavakoli, N.Darmvandi, and R.M.Mazandaran, "Analysis of cross-shaped dual-polarized microstrip patch antennas," in *1995 IEEE AP-S Int. Sym. Dig.*, Newport Beach, CA., June 1995, pp. 994 – 997.
- [8] Ozaki, H.; Ishii, J., "Synthesis of a Class of Strip-Line Filters", *Circuit Theory, IRE Transactions on*, Volume: 5, Issue: 2, Jun 1958, Pages:104 - 109
- [9] Cristal, E.G.; "Coupled-Transmission-Line Directional Couplers with Coupled Lines of Unequal Characteristic Impedances", *Microwave Theory and Techniques, IEEE Transactions on*, Volume: 14, Issue: 7, Jul 1966, Pages:337 – 346
- [10] Thompson, et al. "Characterization of liquid crystal polymer (LCP) material and transmission lines on LCP substrates from 30 to 110 GHz", *MTT, IEEE Transactions on*, Volume: 52, Issue: 4, April 2004, Pages:1343 - 1352